



Manufacturing Science and Education 2026

ACTA TECHNICA NAPOCENSIS

Series: Applied Mathematics, Mechanics, and Engineering  
Vol. 69, Issue I, March, 2026

## DEGRADATION BEHAVIOR OF DIFFERENT MAGNESIUM ALLOYS FOR TEMPORARY IMPLANTS: ROLE OF ALLOYING ELEMENTS, MICROSTRUCTURE, AND TESTING MEDIA

Elena PIEPTEA (Popescu), Aurora ANTONIAC, Iuliana CORNESCHI, Iulian ANTONIAC, Veronica MANESCU (Paltanea), Anca FRATILA

**Abstract:** Biodegradable Mg-based alloys seem to be the future raw materials used for the fabrication of temporary implants used in orthopedic, cardiovascular, dental, and general surgery specializations. The main problem of Mg-based alloys is their faster degradation rate in the human body, which will compromise the biomechanical stability of the implants before the end of the healing process and implicitly increase the tissue healing time. In this study, we investigated how different test media influence the corrosion behavior of magnesium-based alloys. The results obtained indicate that the choice of media significantly influences the corrosion patterns; in particular, simulated body fluid (SBF) is a more corrosive medium. This is due to the high concentration of Cl<sup>-</sup> ions and the absence of organic compounds in the composition.

**Keywords:** Magnesium-based alloy, degradation behavior, Dulbecco's Modified Eagle's Medium, SBF

### 1. INTRODUCTION

Biodegradable alloys based on magnesium, iron, and zinc look to be the future raw materials used for the fabrication of different temporary implants for many medical specializations, like orthopedic, cardiovascular, dental, and general surgery [1–9]. One reason is the failure of the classical medical devices used in different surgical specializations due to the materials and their complications [10–14]. Also, the bifunctional properties of the magnesium-based alloys look very promising: better mechanical properties than other biodegradable materials in use, biodegradability, easy to be metabolized, and positive effects on the cells and tissues [1,2,4]. The main problem of magnesium alloys for surgical implants is their faster degradation rate in the human body, which will compromise the biomechanical stability of the implants before the end of the healing process, and implicitly increase the tissue healing time [15,16]. In this context, in order to optimize the implant's bifunctional properties due to the control of the degradation process of magnesium-based alloys, several methods were developed: new alloying elements for magnesium-based alloys [17–22], new processing methods based mainly on

plastic deformation and heat treatments [23–26], and new surface modification methods [27–37]. The corrosion behavior of magnesium-based materials for medical implants is still a very challenging topic, with different results being obtained according to the *in vivo* and *in vitro* environments [17,38,39]. Also, research groups obtain various results after *in vitro* testing because they use different testing media and different testing conditions [40,41]. In order to increase the similarity of *in vitro* testing media with *in vivo* conditions, researchers include some organic components to increase the complexity of the medium, following some comparative studies between static and dynamic corrosion phenomena, as well as the effect of the hydrogen diffusion coefficient [42].

The development of standardized *in vitro* test methods remains a challenging aspect, as they fail to accurately predict how magnesium-based materials will interact with living tissues, especially when the tissues have different water content [17,43]. However, before performing *in vivo* tests on animals, it is necessary to perform as many *in vitro* tests as possible. In this context, different types of test media with different chemical compositions

have been developed. The test media usually contain inorganic ions, or inorganic ions together with organic compounds. The degradation behavior is different in the case of media containing only inorganic ions compared to those containing also the organic components, like glucose, proteins, and vitamins [44–47]. Experimental results from the literature confirm that the corrosion rate increases with increasing chloride levels in the solution. As an example, SBF (simulated body fluid) contains chlorine ions at concentrations of 147.8 mM, whereas DMEM (Dulbecco's Modified Eagle's Medium) has a concentration of 121 mM, which means a higher corrosion rate is expected in the case of using SBF as a testing medium [48,49]. A selection of the most used testing media for biodegradable magnesium-based alloys is shown in Figure 1, with different complexities in terms of composition. As the chemical complexity of the media increases, its composition becomes more comparable to that of human body fluids (serum/plasma and interstitial fluid) [50].

The objective of the current experimental research was to determine the degradation behavior of different magnesium-based alloys, potentially used for medical implants, in 2 simulated media. The use of corrosive media with a composition similar to that of the internal biological environment for *in vitro* testing enables a more reliable prediction of *in vivo* behavior, resulting in a more accurate assessment of corrosion rate and mechanisms. The corrosive media commonly used in current research include simple isotonic solutions, simulated body fluids, complex saline solutions, cell culture media, and protein-containing media.

Table 1

The chemical composition of the Mg-based alloys							
Alloy code	Composition (wt.%)						
	Zn	Ag	Zr	Y	Ca	Mn	Mg
Alloy1	7.4	1.5	1.0	0.20	-	-	89.90
Alloy2	6.4	2.5	1.0	0.20	-	-	89.90
Alloy3	4.3	-	-	-	0.3	0.62	94.78
Alloy4	-	-	-	-	0.9	-	99.10

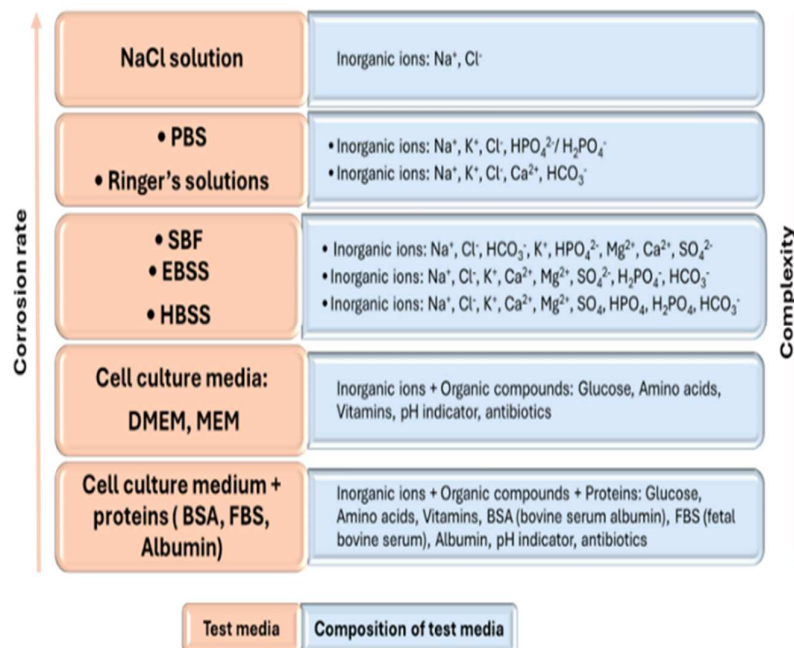


Fig. 1. The current testing media for corrosion evaluation of the biodegradable magnesium-based alloys for potential medical implants

## 2. MATERIALS AND METHODS

The chemical composition of the studied Mg-based alloys is summarized in Table 1. All investigated magnesium-based alloys were produced by the melt casting method. The purpose behind the use of different alloying elements was to follow their

influence on the magnesium-based alloys' microstructure, which is essential for understanding their corrosion behavior. Accordingly, a complex microstructural analysis of the experimental magnesium-based alloys was carried out using optical microscopy (Nikon Metrology Europe, Leuven, Belgium) and scanning electron microscopy

(SEM - ESEM Quattro S Microscope, Thermo Fisher Scientific, Oregon, USA). During the SEM investigations, elemental chemical composition was

For the evaluation of the corrosion behavior of Mg-based alloys, immersion tests were carried out in two different simulated media to determine both the amount of hydrogen released and the mass loss of the samples.

The assessment of hydrogen evolution consists of measuring the volume of hydrogen generated during the immersion of the alloy, which is directly proportional to the quantity of magnesium dissolved from the alloy. The hydrogen release rate (ml/cm<sup>2</sup>) represents the volume of hydrogen released per unit area of the investigated sample surface subjected to the corrosion process and was determined at 24, 48, 72, 96, 120, 144, 168, and 192 hours on five samples of each investigated alloy.

The mass loss was evaluated through the immersion of the experimental alloys in the test medium for various time intervals (24, 48, 72, 96, 120, 144, 168, 192, 216, and 240 hours). Five samples of each investigated alloy type were used for every time point. A thermostatic bath, Julabo Model (DONAU LAB Kft, Budapest, Hungary), was used to maintain the samples at a constant temperature of  $37 \pm 1$  °C. Monitoring the pH of the testing medium was also essential, as the degradation of magnesium alloys leads to the accumulation of HO<sup>-</sup> ions, which shift the solution's pH toward alkaline values, unless stable corrosion products form on the sample surface, inhibiting this process. pH measurements were performed using a HI2210 pH meter (Hanna Instruments, Cluj-Napoca, Romania) at 24, 48, 72, 120, 168, and 92 hours. Mass loss was determined using the following formula:

$$M.L. = \left( \frac{m_0 - m_t}{m_0 - m_t} \right) \times 100$$

where:

$m_0$ – mass of the sample before immersion;

$m_t$ – mass of the sample at different time intervals.

Immersion tests were carried out in Simulated Body Fluid (SBF) and Dulbecco's Modified Eagle's Medium (DMEM), because both of them simulate the composition of human body fluids. Followed Kokubo protocol, we obtained SBF medium using as reagents: potassium chloride (KCl), sodium chloride

measured using energy-dispersive X-ray spectroscopy (EDS; Thermo Fisher Scientific, Oregon, USA).

(NaCl), magnesium chloride hexahydrate (MgCl<sub>2</sub>·6H<sub>2</sub>O), sodium bicarbonate (NaHCO<sub>3</sub>), sodium sulfate (Na<sub>2</sub>SO<sub>4</sub>), potassium phosphate dibasic trihydrate (K<sub>2</sub>HPO<sub>4</sub>·3H<sub>2</sub>O), calcium chloride (CaCl<sub>2</sub>), and 1M hydrochloric acid (HCl) for pH adjustment to 7.4. Dulbecco's medium (pH = 7.0 - 7.6), purchased from Merck (Darmstadt, Germany), contains, in addition to inorganic salts, amino acids, vitamins, and glucose. The Simulated Body Fluid (SBF) uses tris(hydroxymethyl)aminomethane as a buffering agent, while Dulbecco's medium uses 4-(2-hydroxyethyl)piperazine-1-ethane-sulfonic acid (HEPES).

The experimental tests required parallelepiped-shaped samples measuring 15 mm × 15 mm × 5 mm (length × width × height) for precise comparison of the analyzed specimens.

### 3. RESULTS & DISCUSSION

#### 3.1. Microstructural characterization of the experimental magnesium alloys

Optical and SEM-EDS microscopy were used to investigate the microstructural characteristics of four magnesium-based alloys from the Mg-Zn (Alloy 1, Alloy 2, Alloy 3) and Mg-Ca (Alloy 4) systems, with different other alloying elements.

The results obtained are presented in Figures 2 and 3. The microstructure of the investigated samples revealed characteristic features associated with Mg-based alloys casting.

All microstructures exhibit polyhedral  $\alpha$ -Mg grains of various sizes, within which globular compounds can be observed. Precipitates or compounds with different morphologies were identified along the grain boundaries for samples from the Mg-Zn system (Alloy 1, Alloy 2, Alloy 3). In the case of the magnesium alloys from the Mg-Zn system alloyed with different Ag ratios (Alloy 1 and Alloy 2), a decrease in grain size and more pronounced grain boundaries were observed with increasing Ag concentration. In the case of Alloy 4, from the Mg-Ca system, a eutectic structure ( $\alpha$ -Mg + Mg<sub>2</sub>Ca) was identified at the grain boundary.

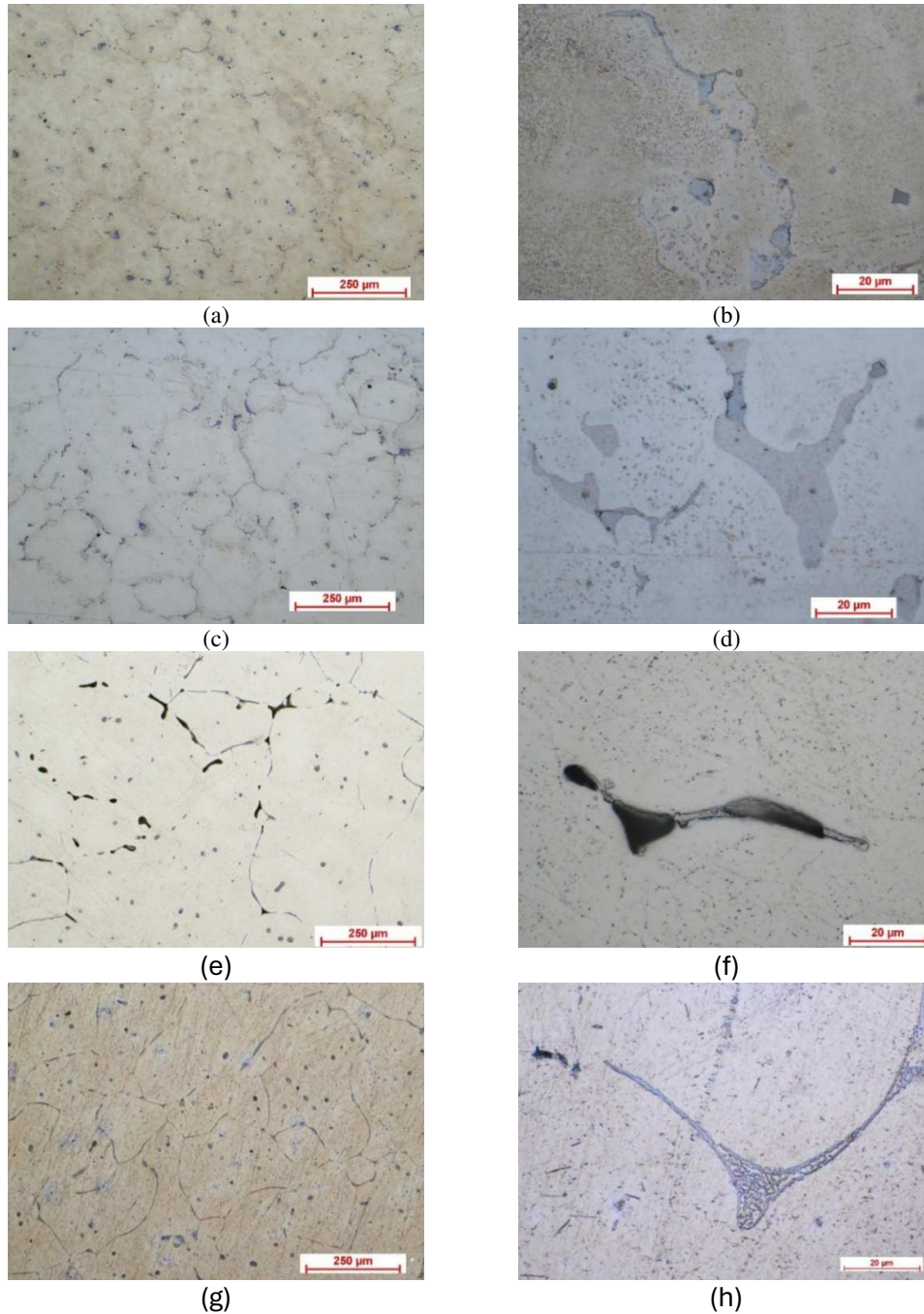
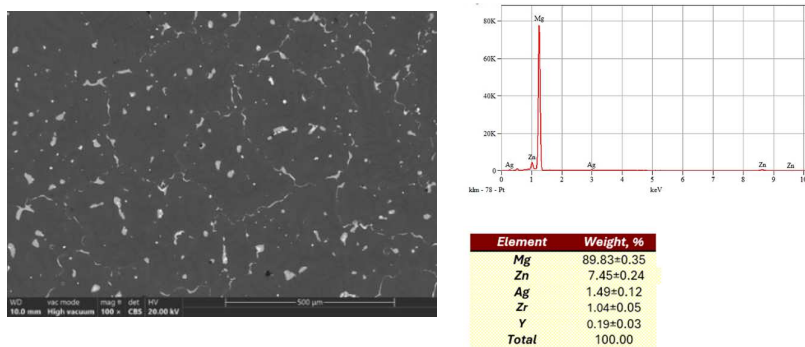


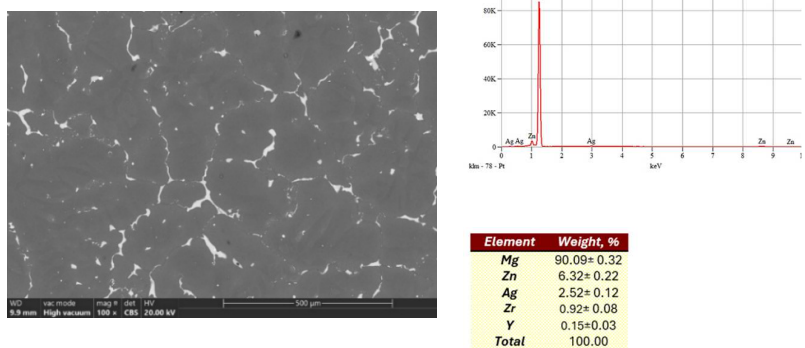
**Fig. 2.** The optical microscopy images (10x and 100x) for: (a) and (b) Alloy 1, (c) and (d) Alloy 2, (e) and (f) Alloy 3, (g) and (h) Alloy 4

As illustrated by the SEM images in Figure 3, the microstructure of the studied magnesium alloys clearly highlights the intermetallic compounds and grain

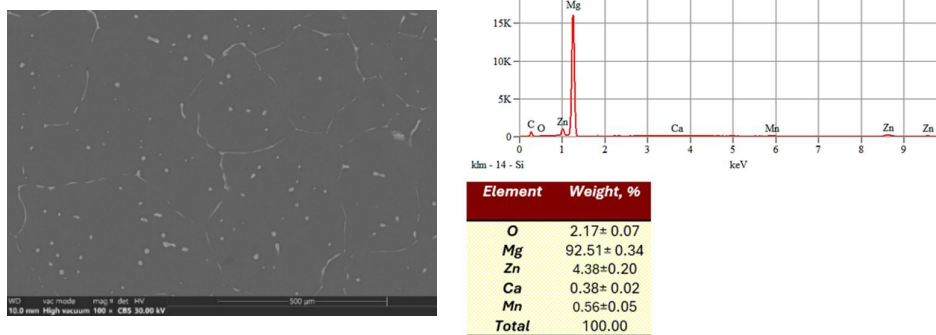
boundaries present in the Mg-based alloys' microstructure.



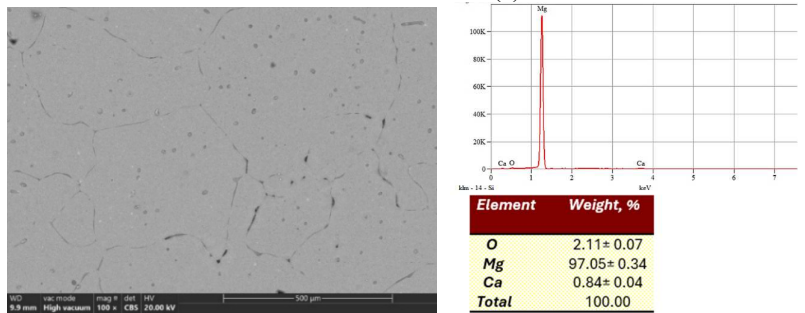
(a)



(b)



(c)



(d)

**Fig. 3.** The scanning electron microscopy images, EDS spectra, and chemical composition for: (a) Alloy 1, (b) Alloy 2, (c) Alloy 3, (d) Alloy 4

The SEM microscopy results confirm the information highlighted by optical microscopy, but

more clearly. In addition, EDS analysis revealed the presence of alloying elements.

For Alloy 3 (which contains 4.3 wt.% Zn) and Alloy 4 (which contains 0.9 wt.% Ca), the presence of elements existing in the composition, as well as the development of a surface oxide layer, denotes a greater susceptibility to oxidation. Also, in the case of Alloy 1 and Alloy 2, the elements Zn, Ag, Zr, and Y were detected in their compositions.

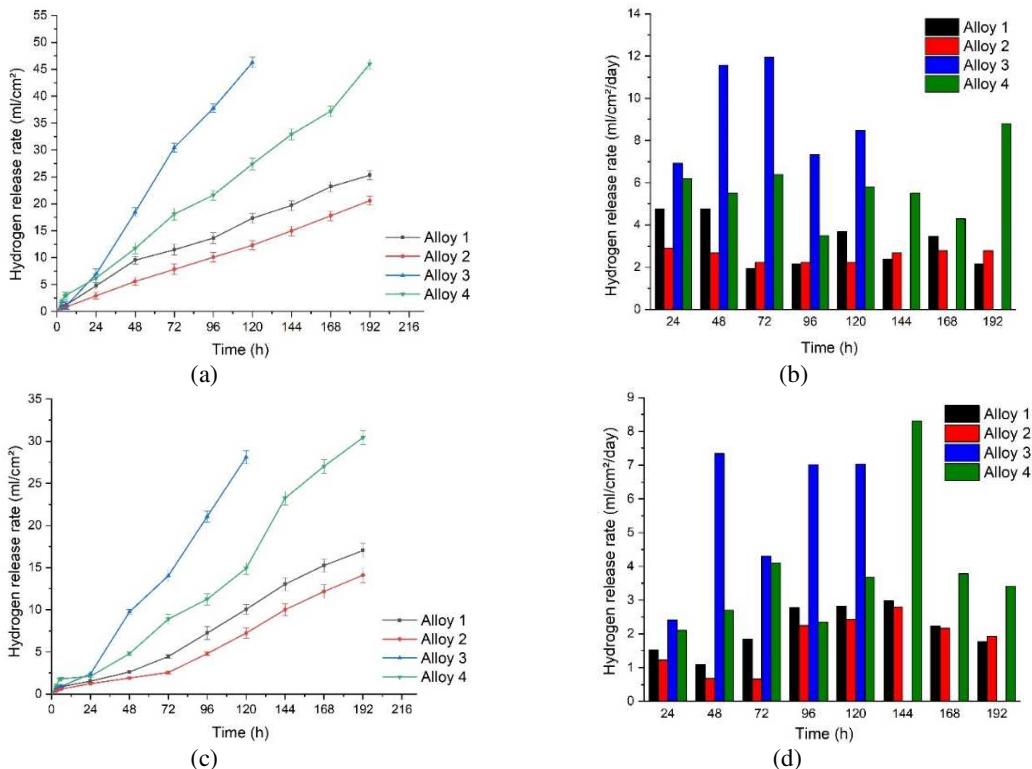
### 3.2. Determination of degradation behavior by immersion testing

Figure 4 shows the evolution of hydrogen release rates for all the investigated Mg-based alloys in two testing media: Simulated Body Fluid (SBF) and Dulbecco's Modified Eagle's Medium (DMEM). The cumulative hydrogen release (ml/cm<sup>2</sup>) and the daily hydrogen release rate (ml/cm<sup>2</sup>/day) over time provide essential information about the corrosion behavior of the alloys.

The best degradation behavior in the SBF environment was observed for Alloy 2 (with 6.4 wt.% Zn and 2.5 wt.% Ag), which had the lowest hydrogen release rate during the test period (up to 192 hours). This was followed by Alloy 1 (with 7.4 wt.% Zn and 1.5 wt.% Ag), Alloy 4 (with 0.9 wt.% Ca), and finally Alloy 3 (with 4.3 wt.% Zn), which

showed the highest hydrogen release rate. These results suggest that silver, especially at higher concentrations, reduces the corrosion rate. This is observed even when the zinc content in the alloy exceeds 4-5 wt.%, a threshold above which zinc is known to negatively influence the corrosion resistance of the alloy [51–53]. At concentrations higher than 4-5 wt.%, Zn tends to form secondary Mg-Zn intermetallic phases, often distributed along grain boundaries, which can act as cathodic sites towards the  $\alpha$ -Mg matrix. This microgalvanic coupling accelerates localized corrosion, especially in chloride-rich environments such as SBF.

Calculation of the daily hydrogen release rate supports the presented observations. Alloy 2 recorded values close to the physiological tolerance limit of the human body (2.25 ml/cm<sup>2</sup>/day), reaching a maximum of 2.90 ml/cm<sup>2</sup>/day. For Alloy 3, it is observed that it significantly exceeded the limit tolerated by the human body, reaching values exceeding 12 ml/cm<sup>2</sup>/day. Alloys 1 and 4 showed intermediate behavior compared to alloys 2 and 3, with values that also exceeded the tolerable limits for the human body.



**Fig. 4.** Hydrogen release rate of the experimental Mg-based alloys in: (a) and (b) SBF Medium; (c) and (d) DMEM

When testing the investigated Mg-based alloys in DMEM medium, lower hydrogen release rates were observed than in SBF medium, indicating that DMEM is less aggressive during the degradation process. Again, Alloy 2 (with 6.4 wt.% Zn and 2.5 wt.% Ag) showed the best evolution, with the lowest cumulative and daily hydrogen release.

The differences between the behavior of the investigated Mg-based alloys in the two media, SBF and DMEM, may be due to their different chemical compositions and the buffer systems they contain. According to the data in the specialized literature, if the concentration of chloride ions,  $\text{Cl}^-$ , in the test medium exceeds a concentration of 30 mM, the magnesium hydroxide layer ( $\text{Mg}(\text{OH})_2$ ) formed on the alloy surface becomes unstable. This is converted into

magnesium chloride ( $\text{MgCl}_2$ ), a salt soluble in the medium [42,54]. Thus, the alloy surface becomes susceptible to corrosion again. As the content of  $\text{Cl}^-$  ions in the SBF medium is 147.8 mM, this explains the obtaining of a higher hydrogen release rate. In addition, the buffer system used in the preparation of the SBF medium, tris(hydroxymethyl)aminomethane, amplifies the degradation by

consuming  $\text{OH}^-$  ions from the medium [55]. In contrast, the slower degradation behavior observed in the DMEM medium can be mainly attributed to the lower  $\text{Cl}^-$  concentration (121 mM), which reduces the decomposition rate of  $\text{Mg}(\text{OH})_2$ .

The evolution of mass loss and pH for the investigated Mg-based alloys in the two testing media is presented in Figure 5.

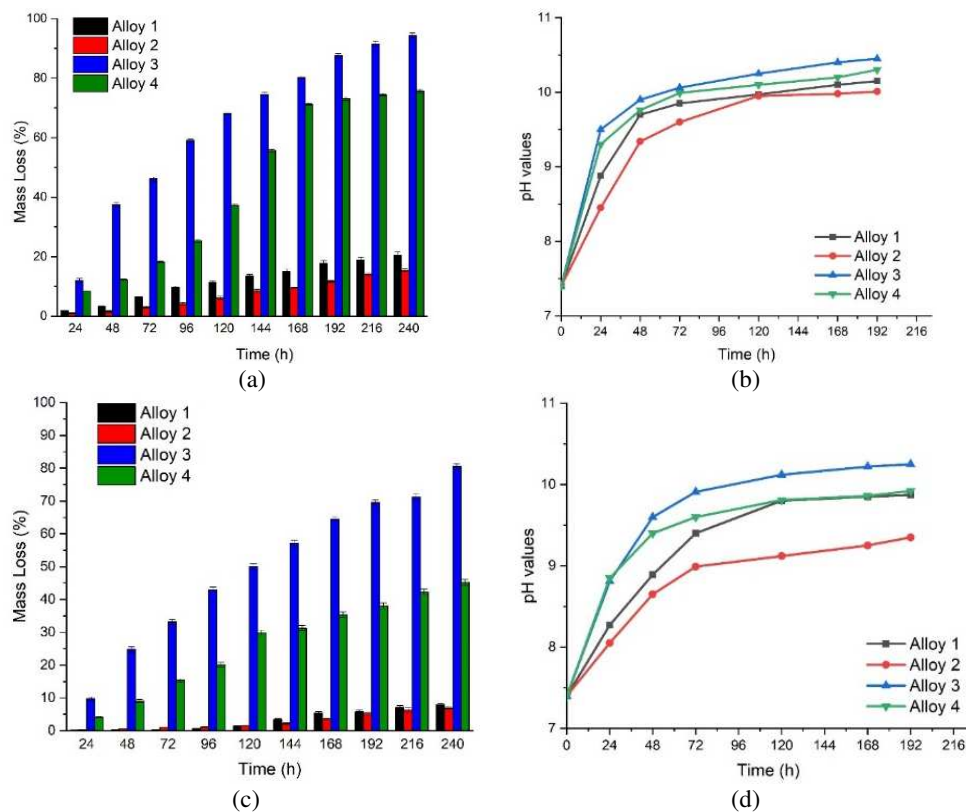


**Fig. 5.** Mass loss and pH evolution of the experimental magnesium-based alloys in: (a) and (b) Simulated Body Fluid Medium; (c) and (d) Dulbecco's Modified Eagle's Medium

The evolution of pH values in both test media confirms the results observed in the mass-loss test. Alloy 3, which showed the highest mass loss, caused the most significant increases in pH in both DMEM and SBF media, exceeding 10.5 in SBF and around 10.2 in DMEM.

This sharp alkalization results from the continuous formation of  $\text{Mg}(\text{OH})_2$  and the subsequent release of  $\text{OH}^-$  ions, a typical by-product of rapid magnesium corrosion.

#### 4. CONCLUSION

In this study, the corrosion process of four magnesium-based alloys was evaluated: 3 from the Mg-Zn system (Alloy 1, Alloy 2, and Alloy 3) and 1 from the Mg-Ca system (Alloy 4). The microstructure of the investigated samples revealed characteristic features associated with Mg-based alloys casting. Even all alloys exhibit polyhedral  $\alpha$ -Mg grains, the grain size and the precipitates or compounds along the grain boundaries are influenced by alloying elements and their concentration. The corrosion mechanism was similar for all experimental alloys. The best degradation behavior was observed for Alloy 2 (with 6.4 wt.% Zn and 2.5 wt.% Ag), which presented the lowest hydrogen release rate, the lowest mass loss, and the most stable pH values in both testing media. The results confirm that the testing media play a critical role in determining corrosion rates. Specifically, the high concentration of Cl<sup>-</sup> ions and the absence of organic compounds make SBF a significantly more corrosive medium for the magnesium alloys studied compared to other media. However, the daily hydrogen release rate and values for mass loss demonstrate that it is necessary to optimize the chemical composition of the studied Mg-based alloys or apply appropriate surface treatments to improve their degradation behavior before being used as raw material for temporary implants.

#### 5. REFERENCES

1. Antoniac, I.; Manescu (Paltanea), V.; Antoniac, A.; Paltanea, G. Magnesium-Based Alloys with Adapted Interfaces for Bone Implants and Tissue Engineering. *Regen Biomater* 2023, 10, doi:10.1093/rb/rbad095.
2. Zheng, Y.F.; Gu, X.N.; Witte, F. Biodegradable Metals. *Materials Science and Engineering: R: Reports* 2014, 77, 1–34, doi:10.1016/j.mser.2014.01.001.
3. Bitu, A.I.; A.I., C.I. Potential Use of Mg-Ca Alloys for Orthopedic Applications. *U.P.B. Sci. Bull., Series B* 2016, 78.
4. Mueller, W.-D.; Lucia Nascimento, M.; Lorenzo de Mele, M.F. Critical Discussion of the Results from Different Corrosion Studies of Mg and Mg Alloys for Biomaterial Applications☆. *Acta Biomater* 2010, 6, 1749–1755, doi:10.1016/j.actbio.2009.12.048.
5. Manescu (Paltanea), V.; Antoniac, I.; Antoniac, A.; Laptou, D.; Paltanea, G.; Ciocoiu, R.; Nemoianu, I.V.; Gruionu, L.G.; Dura, H. Bone Regeneration Induced by Patient-Adapted Mg Alloy-Based Scaffolds for Bone Defects: Present and Future Perspectives. *Biomimetics* 2023, 8, 618, doi:10.3390/biomimetics8080618.
6. Gu, X.; Zheng, Y.; Cheng, Y.; Zhong, S.; Xi, T. In Vitro Corrosion and Biocompatibility of Binary Magnesium Alloys. *Biomaterials* 2009, 30, 484–498, doi:10.1016/j.biomaterials.2008.10.021.
7. Zhao, D.; Witte, F.; Lu, F.; Wang, J.; Li, J.; Qin, L. Current Status on Clinical Applications of Magnesium-Based Orthopaedic Implants: A Review from Clinical Translational Perspective. *Biomaterials* 2017, 112, 287–302, doi:10.1016/j.biomaterials.2016.10.017.
8. Mostaed, E.; Sikora-Jasinska, M.; Drelich, J.W.; Vedani, M. Zinc-Based Alloys for Degradable Vascular Stent Applications. *Acta Biomater* 2018, 71, 1–23, doi:10.1016/j.actbio.2018.03.005.
9. Han, H.-S.; Loffredo, S.; Jun, I.; Edwards, J.; Kim, Y.-C.; Seok, H.-K.; Witte, F.; Mantovani, D.; Glyn-Jones, S. Current Status and Outlook on the Clinical Translation of Biodegradable Metals. *Materials Today* 2019, 23, 57–71, doi:10.1016/j.mattod.2018.05.018.
10. Rodica, M.; Iulian, A.; Dan, L.; Aurora, A.; Dan, G. Complications Related to Biocomposite Screw Fixation in ACL Reconstruction Based on Clinical Experience and Retrieval Analysis. *Materiale Plastice* 2015, 52.
11. Craciunescu, E.; Sinescu, C.; Negrutiu, M.L.; Pop, D.M.; Lauer, H.-C.; Rominu, M.; Hutiu, G.; Bunoiu, M.; Duma, V.-F.; Antoniac, I. Shear Bond Strength Tests of Zirconia Veneering Ceramics after Chipping Repair. *J Adhes Sci Technol* 2016, 30, 666–676, doi:10.1080/01694243.2015.1117304.
12. Antoniac, I.; Negrusoiu, M.; Mardare, M.; Socoliuc, C.; Zazyva, A.; Niculescu, M.

- Adverse Local Tissue Reaction after 2 Revision Hip Replacements for Ceramic Liner Fracture. *Medicine* 2017, 96, e6687, doi:10.1097/MD.0000000000006687.
13. Nica, M.; Cretu, B.; Ene, D.; Antoniac, I.; Gheorghita, D.; Ene, R. Failure Analysis of Retrieved Osteosynthesis Implants. *Materials* 2020, 13, 1201, doi:10.3390/ma13051201.
  14. Mavrodin, C.I.; Pariza, G.; Ion, D.; Antoniac, V.I. Abdominal Compartment Syndrome -- a Major Complication of Large Incisional Hernia Surgery. *Chirurgia (Bucur)* 2013, 108, 414–417.
  15. Chen, Y.; Xu, Z.; Smith, C.; Sankar, J. Recent Advances on the Development of Magnesium Alloys for Biodegradable Implants. *Acta Biomater* 2014, 10, 4561–4573, doi:10.1016/j.actbio.2014.07.005.
  16. Zhang, T.; Wang, W.; Liu, J.; Wang, L.; Tang, Y.; Wang, K. A Review on Magnesium Alloys for Biomedical Applications. *Front Bioeng Biotechnol* 2022, 10, doi:10.3389/fbioe.2022.953344.
  17. Witte, F.; Fischer, J.; Nellesen, J.; Crostack, H.-A.; Kaese, V.; Pisch, A.; Beckmann, F.; Windhagen, H. In Vitro and in Vivo Corrosion Measurements of Magnesium Alloys. *Biomaterials* 2006, 27, 1013–1018, doi:10.1016/j.biomaterials.2005.07.037.
  18. Jiang, P.; Blawert, C.; Hou, R.; Scharnagl, N.; Bohlen, J.; Zheludkevich, M.L. Microstructural Influence on Corrosion Behavior of MgZnGe Alloy in NaCl Solution. *J Alloys Compd* 2019, 783, 179–192, doi:10.1016/j.jallcom.2018.12.296.
  19. Li, N.; Zheng, Y. Novel Magnesium Alloys Developed for Biomedical Application: A Review. *J Mater Sci Technol* 2013, 29, 489–502, doi:10.1016/j.jmst.2013.02.005.
  20. Hort, N.; Huang, Y.; Fechner, D.; Störmer, M.; Blawert, C.; Witte, F.; Vogt, C.; Drücker, H.; Willumeit, R.; Kainer, K.U. Magnesium Alloys as Implant Materials – Principles of Property Design for Mg–RE Alloys☆. *Acta Biomater* 2010, 6, 1714–1725, doi:10.1016/j.actbio.2009.09.010.
  21. Qin, H.; Zhao, Y.; An, Z.; Cheng, M.; Wang, Q.; Cheng, T.; Wang, Q.; Wang, J.; Jiang, Y.; Zhang, X.; et al. Enhanced Antibacterial Properties, Biocompatibility, and Corrosion Resistance of Degradable Mg–Nd–Zn–Zr Alloy. *Biomaterials* 2015, 53, 211–220, doi:10.1016/j.biomaterials.2015.02.096.
  22. Wang, J.-L.; Mukherjee, S.; Nisbet, D.R.; Birbilis, N.; Chen, X.-B. In Vitro Evaluation of Biodegradable Magnesium Alloys Containing Micro-Alloying Additions of Strontium, with and without Zinc. *J Mater Chem B* 2015, 3, 8874–8883, doi:10.1039/C5TB01516B.
  23. Zhang, C.Z.; Zhu, S.J.; Wang, L.G.; Guo, R.M.; Yue, G.C.; Guan, S.K. Microstructures and Degradation Mechanism in Simulated Body Fluid of Biomedical Mg–Zn–Ca Alloy Processed by High Pressure Torsion. *Mater Des* 2016, 96, 54–62, doi:10.1016/j.matdes.2016.01.072.
  24. Song, G.-L.; Xu, Z. Effect of Microstructure Evolution on Corrosion of Different Crystal Surfaces of AZ31 Mg Alloy in a Chloride Containing Solution. *Corros Sci* 2012, 54, 97–105, doi:10.1016/j.corsci.2011.09.005.
  25. Zhang, W.; Tan, L.; Ni, D.; Chen, J.; Zhao, Y.-C.; Liu, L.; Shuai, C.; Yang, K.; Atrens, A.; Zhao, M.-C. Effect of Grain Refinement and Crystallographic Texture Produced by Friction Stir Processing on the Biodegradation Behavior of a Mg–Nd–Zn Alloy. *J Mater Sci Technol* 2019, 35, 777–783, doi:10.1016/j.jmst.2018.11.025.
  26. Wang, J.; Zhou, Y.; Yang, Z.; Zhu, S.; Wang, L.; Guan, S. Processing and Properties of Magnesium Alloy Micro-Tubes for Biodegradable Vascular Stents. *Materials Science and Engineering: C* 2018, 90, 504–513, doi:10.1016/j.msec.2018.05.005.
  27. Feng, Y.; Ma, X.; Chang, L.; Zhu, S.; Guan, S. Characterization and Cytocompatibility of Polydopamine on MAO–HA Coating Supported on Mg–Zn–Ca Alloy. *Surface and Interface Analysis* 2017, 49, 1115–1123, doi:10.1002/sia.6286.

28. Dragomir (Nicolescu), L.; Antoniac, A.; Manescu (Paltanea), V.; Robu, A.; Dinu, M.; Pana, I.; Cotrut, C.M.; Kamel, E.; Antoniac, I.; Rau, J. V.; et al. Preparation and Characterization of Hydroxyapatite Coating by Magnetron Sputtering on Mg–Zn–Ag Alloys for Orthopaedic Trauma Implants. *Ceram Int* 2023, 49, 26274–26288, doi:10.1016/j.ceramint.2023.05.116.
29. Hornberger, H.; Virtanen, S.; Boccaccini, A.R. Biomedical Coatings on Magnesium Alloys – A Review. *Acta Biomater* 2012, 8, 2442–2455, doi:10.1016/j.actbio.2012.04.012.
30. Bița, A.-I.; Antoniac, I.; Miculescu, M.; Stan, G.E.; Leonat, L.; Antoniac, A.; Constantin, B.; Fornă, N. Electrochemical and In Vitro Biological Evaluation of Bio-Active Coatings Deposited by Magnetron Sputtering onto Biocompatible Mg-0.8Ca Alloy. *Materials* 2022, 15, 3100, doi:10.3390/ma15093100.
31. Quan, P.H.; Antoniac, I.; Miculescu, F.; Antoniac, A.; (Păltânea), V.M.; Robu, A.; Bița, A.-I.; Miculescu, M.; Săceleanu, A.; Bodog, A.D.; et al. Fluoride Treatment and In Vitro Corrosion Behavior of Mg–Nd–Y–Zn–Zr Alloys Type. *Materials* 2022, 15, 566, doi:10.3390/ma15020566.
32. Chen, Y.; Lu, X.; Lamaka, S. V.; Ju, P.; Blawert, C.; Zhang, T.; Wang, F.; Zheludkevich, M.L. Active Protection of Mg Alloy by Composite PEO Coating Loaded with Corrosion Inhibitors. *Appl Surf Sci* 2020, 504, 144462, doi:10.1016/j.apsusc.2019.144462.
33. Streza, A.; Antoniac, A.; Manescu (Paltanea), V.; Paltanea, G.; Robu, A.; Dura, H.; Verestiuc, L.; Stanica, E.; Voicu, S.I.; Antoniac, I.; et al. Effect of Filler Types on Cellulose-Acetate-Based Composite Used as Coatings for Biodegradable Magnesium Implants for Trauma. *Materials* 2023, 16, 554, doi:10.3390/ma16020554.
34. Wang, H.X.; Guan, S.K.; Wang, X.; Ren, C.X.; Wang, L.G. In Vitro Degradation and Mechanical Integrity of Mg–Zn–Ca Alloy Coated with Ca-Deficient Hydroxyapatite by the Pulse Electrodeposition Process☆. *Acta Biomater* 2010, 6, 1743–1748, doi:10.1016/j.actbio.2009.12.009.
35. Rau, J.V.; Antoniac, I.; Filipescu, M.; Cotrut, C.; Fosca, M.; Nistor, L.C.; Birjega, R.; Dinescu, M. Hydroxyapatite Coatings on Mg–Ca Alloy Prepared by Pulsed Laser Deposition: Properties and Corrosion Resistance in Simulated Body Fluid. *Ceram Int* 2018, 44, 16678–16687, doi:10.1016/j.ceramint.2018.06.095.
36. Mohedano, M.; Luthringer, B.J.C.; Mingo, B.; Feyerabend, F.; Arrabal, R.; Sanchez-Egido, P.J.; Blawert, C.; Willumeit-Römer, R.; Zheludkevich, M.L.; Matykina, E. Bioactive Plasma Electrolytic Oxidation Coatings on Mg–Ca Alloy to Control Degradation Behaviour. *Surf Coat Technol* 2017, 315, 454–467, doi:10.1016/j.surfcoat.2017.02.050.
37. Rau, J.V.; Antoniac, I.; Fosca, M.; De Bonis, A.; Blajan, A.I.; Cotrut, C.; Graziani, V.; Curcio, M.; Cricenti, A.; Nicolescu, M.; et al. Glass-Ceramic Coated Mg–Ca Alloys for Biomedical Implant Applications. *Materials Science and Engineering: C* 2016, 64, 362–369, doi:10.1016/j.msec.2016.03.100.
38. Staiger, M.P.; Feyerabend, F.; Willumeit, R.; Sfeir, C.S.; Zheng, Y.F.; Virtanen, S.; Müller, W.D.; Atrens, A.; Peuster, M.; Kumta, P.N.; et al. Summary of the Panel Discussions at the 2nd Symposium on Biodegradable Metals, Maratea, Italy, 2010. *Materials Science and Engineering: B* 2011, 176, 1596–1599, doi:10.1016/j.mseb.2011.09.032.
39. Mei, D.; Lamaka, S. V.; Gonzalez, J.; Feyerabend, F.; Willumeit-Römer, R.; Zheludkevich, M.L. The Role of Individual Components of Simulated Body Fluid on the Corrosion Behavior of Commercially Pure Mg. *Corros Sci* 2019, 147, 81–93, doi:10.1016/j.corsci.2018.11.011.
40. A.I. Bița; A. Antoniac; C. Cotrut; E. Vasile; I. Ciuca; M. Nicolescu; I. Antoniac; In Vitro Degradation and Corrosion Evaluation of Mg–Ca Alloys for Biomedical Applications. *Journal of Optoelectronics and Advanced Materials* 2016, 18, 394–398.

41. Wang, H.; Shi, Z. *In Vitro* Biodegradation Behavior of Magnesium and Magnesium Alloy. *J Biomed Mater Res B Appl Biomater* 2011, *98B*, 203–209, doi:10.1002/jbm.b.31769.
42. Witte, F.; Hort, N.; Vogt, C.; Cohen, S.; Kainer, K.U.; Willumeit, R.; Feyerabend, F. Degradable Biomaterials Based on Magnesium Corrosion. *Curr Opin Solid State Mater Sci* 2008, *12*, 63–72, doi:10.1016/j.cossms.2009.04.001.
43. Sanchez, A.H.M.; Luthringer, B.J.C.; Feyerabend, F.; Willumeit, R. Mg and Mg Alloys: How Comparable Are *In Vitro* and *In Vivo* Corrosion Rates? A Review. *Acta Biomater* 2015, *13*, 16–31, doi:10.1016/j.actbio.2014.11.048.
44. Kuwahara, H.; Al-Abdullat, Y.; Mazaki, N.; Tsutsumi, S.; Aizawa, T. Precipitation of Magnesium Apatite on Pure Magnesium Surface during Immersing in Hank&rsquo;s Solution. *Mater Trans* 2001, *42*, 1317–1321, doi:10.2320/matertrans.42.1317.
45. Müller, W.D.; Nascimento, M.L.; Zeddies, M.; Córscico, M.; Gassa, L.M.; Mele, M.A.F.L. de Magnesium and Its Alloys as Degradable Biomaterials: Corrosion Studies Using Potentiodynamic and EIS Electrochemical Techniques. *Materials Research* 2007, *10*, 5–10, doi:10.1590/S1516-14392007000100003.
46. Witte, F.; Kaese, V.; Haferkamp, H.; Switzer, E.; Meyer-Lindenberg, A.; Wirth, C.J.; Windhagen, H. *In Vivo* Corrosion of Four Magnesium Alloys and the Associated Bone Response. *Biomaterials* 2005, *26*, 3557–3563, doi:10.1016/j.biomaterials.2004.09.049.
47. Kaya, R.A.; Çavuşoğlu, H.; Tanik, C.; Kaya, A.A.; Duygulu, Ö.; Mutlu, Z.; Zengin, E.; Aydin, Y. The Effects of Magnesium Particles in Posterolateral Spinal Fusion: An Experimental *In Vivo* Study in a Sheep Model. *J Neurosurg Spine* 2007, *6*, 141–149, doi:10.3171/spi.2007.6.2.141.
48. Rohanová, D.; Boccaccini, A.R.; Horkavcová, D.; Bozděchová, P.; Bezdička, P.; Častorálová, M. Is Non-Buffered DMEM Solution a Suitable Medium for *In Vitro* Bioactivity Tests? *J. Mater. Chem. B* 2014, *2*, 5068–5076, doi:10.1039/C4TB00187G.
49. Kokubo, T.; Takadama, H. How Useful Is SBF in Predicting *In Vivo* Bone Bioactivity? *Biomaterials* 2006, *27*, 2907–2915, doi:10.1016/j.biomaterials.2006.01.017.
50. Mei, D.; Lamaka, S. V.; Lu, X.; Zheludkevich, M.L. Selecting Medium for Corrosion Testing of Bioabsorbable Magnesium and Other Metals – A Critical Review. *Corros Sci* 2020, *171*, 108722, doi:10.1016/j.corsci.2020.108722.
51. Song, Y.; Han, E.-H.; Shan, D.; Yim, C.D.; You, B.S. The Role of Second Phases in the Corrosion Behavior of Mg–5Zn Alloy. *Corros Sci* 2012, *60*, 238–245, doi:10.1016/j.corsci.2012.03.030.
52. Ding, Y.; Wen, C.; Hodgson, P.; Li, Y. Effects of Alloying Elements on the Corrosion Behavior and Biocompatibility of Biodegradable Magnesium Alloys: A Review. *J. Mater. Chem. B* 2014, *2*, 1912–1933, doi:10.1039/C3TB21746A.
53. Koç, E.; Kannan, M.B.; Ünal, M.; Candan, E. Influence of Zinc on the Microstructure, Mechanical Properties and *In Vitro* Corrosion Behavior of Magnesium–Zinc Binary Alloys. *J Alloys Compd* 2015, *648*, 291–296, doi:10.1016/j.jallcom.2015.06.227.
54. Neves, C.S.; Sousa, I.; Freitas, M.A.; Moreira, L.; Costa, C.; Teixeira, J.P.; Fraga, S.; Pinto, E.; Almeida, A.; Scharnagl, N.; et al. Insights into Corrosion Behaviour of Uncoated Mg Alloys for Biomedical Applications in Different Aqueous Media. *Journal of Materials Research and Technology* 2021, *13*, 1908–1922, doi:10.1016/j.jmrt.2021.05.090.
55. Xin, Y.; Hu, T.; Chu, P.K. Influence of Test Solutions on *In Vitro* Studies of Biomedical Magnesium Alloys. *J Electrochem Soc* 2010, *157*, C238, doi:10.1149/1.3421651.
56. Wang, Y.; Ding, B.-H.; Gao, S.-Y.; Chen, X.-B.; Zeng, R.-C.; Cui, L.-Y.; Li, S.-J.; Li, S.-Q.; Zou, Y.-H.; Han, E.-H.; et al. *In Vitro* Corrosion of Pure Mg in Phosphate Buffer Solution—Influences of Isoelectric Point and

- Molecular Structure of Amino Acids. *Materials Science and Engineering: C* 2019, 105, 110042, doi:10.1016/j.msec.2019.110042.
57. Fang, Z.; Wang, J.; Yang, X.; Sun, Q.; Jia, Y.; Liu, H.; Xi, T.; Guan, S. Adsorption of Arginine, Glycine and Aspartic Acid on Mg and Mg-Based Alloy Surfaces: A First-Principles Study. *Appl Surf Sci* 2017, 409, 149–155, doi:10.1016/j.apsusc.2017.02.241.
58. Helal, N.H.; Badawy, W.A. Environmentally Safe Corrosion Inhibition of Mg–Al–Zn Alloy in Chloride Free Neutral Solutions by Amino Acids. *Electrochim Acta* 2011, 56, 6581–6587, doi:10.1016/j.electacta.2011.04.031.

### Comportamentul la degradare a diferitelor aliaje de magneziu pentru implanturi temporare: rolul elementelor de aliere, microstructurii și mediilor de testare

*Aliajele biodegradabile pe bază de Mg par a fi viitoarele materii prime utilizate pentru fabricarea implanturilor temporare utilizate în specializările ortopedice, cardiovasculare, stomatologice și chirurgie generală. Principala problemă a aliajelor pe bază de Mg este rata de degradare rapidă în corpul uman, ceea ce va compromite stabilitatea biomecanică a implanturilor înainte de sfârșitul procesului de vindecare și implicit va crește timpul de vindecare a țesuturilor. Obiectivul cercetării experimentale actuale a fost de a determina efectul mediilor de testare asupra comportamentului la coroziune al diferitelor aliaje pe bază de Mg. Investigațiile privind comportamentul la coroziune demonstrează că mediile de testare au o influență puternică, fluidul corporal simulat (SBF) fiind un mediu mai coroziv datorită prezenței unei concentrații mai mari de ioni de Cl și absenței compușilor organici în compoziția sa.*

**Cuvinte cheie:** aliaj de magneziu, degradare, fluidul corporal simulat, Mediul Eagle modificat de Dulbecco (DMEM)

**Elena PIEPTEA (Popescu)**, PhD Student, Faculty of Materials Science and Engineering, National University of Science and Technology POLITEHNICA Bucharest, Romania, e-mail: elena\_eli.popescu@upb.ro

**Aurora ANTONIAC**, Researcher, Faculty of Materials Science and Engineering, National University of Science and Technology POLITEHNICA Bucharest, Romania, e-mail: aurora.antoniac@upb.ro

**Iuliana CORNESCHI**, Student, Faculty of Materials Science and Engineering, National University of Science and Technology POLITEHNICA Bucharest, Romania, e-mail: iuliana.corneschi@stud.sim.upb.ro

**Iulian ANTONIAC**, Prof., Faculty of Materials Science and Engineering, National University of Science and Technology POLITEHNICA Bucharest, Romania, e-mail: iulian.antoniac@upb.ro; Prof., Academy of Romanian Scientists, Bucharest, Romania

**Veronica MANESCU (Paltanea)**, PhD Student, Faculty of Materials Science and Engineering, National University of Science and Technology POLITEHNICA Bucharest, Romania, e-mail: veronica.paltanea@upb.ro; Assoc. Prof., Faculty of Electrical Engineering, National University of Science and Technology POLITEHNICA Bucharest, Romania

**Anca FRATILA**, Lect., Faculty of Medicine, Lucian Blaga University of Sibiu, Romania; e-mail: anca.fratila@ulbsibiu.ro